Acid-Base Transport by the Renal Proximal Tubule

Walter F. Boron

Department of Cellular and Molecular Physiology, Yale University School of Medicine, New Haven, Connecticut

One of the major tasks of the renal proximal tubule is to secrete acid into the tubule lumen, thereby reabsorbing approximately 80% of the filtered HCO_3^- as well as generating new HCO_3^- for regulating blood pH. This review summarizes the cellular and molecular events that underlie four major processes in HCO_3^- reabsorption. The first is CO_2 entry across the apical membrane, which in large part occurs *via* a gas channel (aquaporin 1) and acidifies the cell. The second process is apical H^+ secretion *via* Na-H exchange and H^+ pumping, processes that can be studied using the NH_4^+ prepulse technique. The third process is the basolateral exit of HCO_3^- *via* the electrogenic Na/HCO_3 co-transporter, which is the subject of at least 10 mutations that cause severe proximal renal tubule acidosis in humans. The final process is the regulation of overall HCO_3^- reabsorption by CO_2 and HCO_3^- sensors at the basolateral membrane. Together, these processes ensure that the proximal tubule responds appropriately to acute acid-base disturbances and thereby contributes to the regulation of blood pH.

J Am Soc Nephrol 17: 2368–2382, 2006. doi: 10.1681/ASN.2006060620

At the outset, allow me to acknowledge my mentors, without whom I would never have been in the position to summarize my Homer W. Smith Award Lecture. One limb of my scientific family tree is decidedly nonrenal: I did my Ph.D. research and 1 yr of postdoctoral work with Albert Roos (a respiratory physiologist) in the Department of Physiology and Biophysics at Washington University in St. Louis. There, I learned to think critically and to begin to understand acid-base physiology. At the same time, Paul De Weer (a biophysicist/neurophysiologist) took me under his wing during summers in Woods Hole. There, I became acquainted with the squid giant axon and the concept of transient changes in voltage and pH. Also at Woods Hole, I was befriended by John M. Russell. In our collaborations, I learned to think about links between HCO_3^- fluxes on the one hand and Na^+ and Cl^- fluxes on the other.

The other limb of my scientific family tree is of course quite renal. I studied for two years as a fellow with Emile Boulpaep in the Department of Physiology (now, of course, Cellular and Molecular Physiology). There, I learned to think about kidneys and to perfuse renal tubules. Emile (1986 Homer W. Smith Award) was trained by Gerhard Giebisch (1971 Homer W. Smith Award), who in turn was trained by Robert Pitts (1964 Homer W. Smith Award), who in turn was trained by Homer W. Smith himself. Smith was trained by Walter B. Cannon, who originated the concept of homeostasis. In fact, while with Cannon, Smith studied—of all things—intracellular pH (pH_i). I suppose that with such an auspicious list forebears, I had no choice but to study acid-base homeostasis. My group is interested in how the body, by controlling plasma [HCO_3^-] and Pco_2, regulates blood pH. One focus is the proximal tubule (PT), which, along with the rest of the kidney, is largely responsible for controlling plasma [HCO_3^-]. A parallel focus is the regulation of pH_i by central nervous system neurons, which regulate ventilation, which in turn controls plasma Pco_2. Along the way, we stumbled across the concept of gas channels, which seem to be important for both respiration and acid-base homeostasis. In this review, I summarize some renal aspects of our work.

The PT is responsible for reabsorbing approximately 80% of the filtered HCO_3^-. The PT also creates the "new HCO_3^-" that neutralizes the mineral acids that are generated by metabolism. The thick ascending limb reabsorbs another 10% of the filtered HCO_3^-, and the distal nephron another approximately 10%, so virtually no HCO_3^- is left in the final urine. Regardless of whether the PT is reabsorbing HCO_3^- or creating new HCO_3^-, the fundamental mechanism (Figure 1) is the same (1–3): PT cells use the cytosolic enzyme carbonic anhydrase II (CA II) to convert CO_2 and H_2O to H^+ and HCO_3^- (4). Mutations in CA II produce a proximal renal tubule acidosis (pRTA). The cells secrete the H^+ into the tubule lumen, *via* the apical Na-H exchanger NHE3 (5–8) and V-type H^+ pumps (9,10). The cells move the HCO_3^- into the interstitial fluid and ultimately the blood, mainly *via* the renal splice variant of the electrogenic Na/HCO_3 co-transporter NBCe1-A (11,12).

Most of the H^+ that the PT secretes into the lumen titrates filtered HCO_3^-, forming CO_2 and H_2O under the influence of CA IV (4), which is tethered to the apical membrane. The H_2O crosses the apical membrane almost exclusively *via* the water channel aquaporin 1 (AQP1) (13), and this same protein—now acting like a gas channel—seems to mediate the majority of CO_2 transport as well. The net effect of the processes that we have summarized is $NaHCO_3$ reabsorption.

A small fraction of the H^+ that the PT secretes into the lumen titrates a variety of luminal buffers (*e.g.*, NH_3, inorganic phosphate, creatinine), which we measure as NH_4^+ excretion and

Published online ahead of print. Publication date available at www.jasn.org.

Address correspondence to: Dr. Walter F. Boron, Department of Cellular and Molecular Physiology, Yale University School of Medicine, 333 Cedar Street, New Haven, CT 06520-8026. Phone: 203-785-4070; Fax: 203-785-4951; E-mail: walter.boron@yale.edu

ISSN: 1046-6673/1709-2368

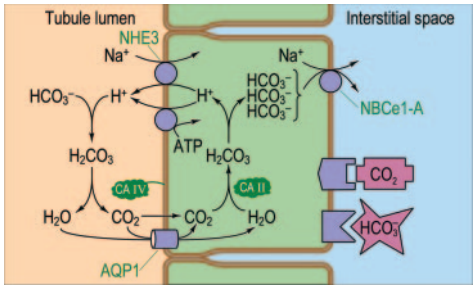

Figure 1. Model of acid-base transport in the proximal tubule (PT). The PT reabsorbs HCO_3^- by using active-transport processes to secrete H^+ into the tubule lumen and titrating HCO_3^- to CO_2 and H_2O. Thus, HCO_3^- reabsorption requires CO_2 uptake across the apical membrane. Once inside the cell, CO_2 and H_2O recombine to regenerate HCO_3^-, which exits across the basolateral membrane. NHE3, Na-H exchanger 3; AQP1, aquaporin 1; CA II and CA IV, carbonic anhydrases II and IV; NBCe1-A, electrogenic Na/HCO_3 co-transporter 1, splice variant A.

the formation of titratable acid (14). The tiny amount of HCO_3^- that, in parallel, moves into the blood is the "new HCO_3^-."

In this review, for the sake of simplicity, I refer to PT transepithelial acid-base transport as "HCO_3^- reabsorption" ($JHCO_3$). In fact, I mean the sum of $JHCO_3$ and the creation of new HCO_3^-. We will see that these processes are under the powerful control of a system that we are only beginning to understand, one that acutely monitors plasma [CO_2] and [HCO_3^-] but not plasma pH.

Apical CO_2 Entry

Effect of CO_2 on pH_i

Since the work of Jacobs on *Symphytum* flower petals (the pigment of which is a pH indicator) in 1920 (15), it has been appreciated that CO_2 can rapidly cross cell membranes and acidify the cytoplasm (reviewed in reference [16]). Thomas (17) and Boron and De Weer (18), both working with pH-sensitive microelectrodes, did the first work with physiologic levels of CO_2 on animal cells. Both studies confirmed that CO_2 does indeed cause a rapid fall in pH_i (Figure 2A), as shown for the squid axon by the initial part of the record in Figure 2B. If CO_2 simply equilibrated across the cell membrane, as shown in Figure 2A, then pH_i would have fallen—by an amount determined by the initial pH_i, [CO_2], and intracellular buffering power (16,19,20)—and stabilized. However, pH_i recovers from this acute acid load *via* a mechanism that requires the input of energy. The experiment in Figure 2B was the first to demonstrate such a pH_i recovery, that is, dynamic pH_i regulation. We now know that a Na^+-driven Cl-HCO_3 exchanger (discussed below) is responsible for this pH_i recovery—a metabolic compensation (*i.e.*, HCO_3^- uptake) to a respiratory acidosis (*i.e.*, CO_2 influx). The withdrawal of CO_2 causes pH_i to rise substantially above its initial level, this overshoot being a direct reflection of the preceding metabolic compensation. Subsequent work by scores of authors on countless cell types, including the PT and other renal cells, shows that the response of virtually all cells

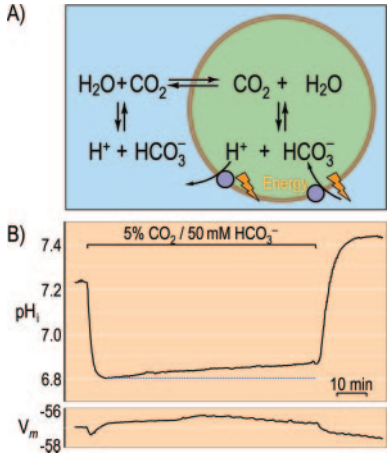

Figure 2. Recovery of pH_i from a CO_2-induced acid load. (A) Model of CO_2 equilibration across the cell membrane. Either the extrusion of H^+ or the uptake of HCO_3^- would require energy. (B) Experimental record from a squid giant axon. The axon was cannulated at either end, and a glass, pH-sensitive microelectrode was inserted from one end, and a KCl-filled microelectrode was inserted from the other. pH_i, intracellular pH; V_m, membrane potential (in mV). Data from reference (18).

to CO_2/HCO_3^- is some variation on the theme first demonstrated with the squid giant axon (for review, see reference [21]).

Membranes with Negligible Gas Permeability

One of the core dogmas of physiology has been that all gases rapidly cross all membranes by dissolving in the membrane lipid. In the case of CO_2, the gas produces the effects that are shown in Figure 2B. For example, perfusing the lumen of a PT with CO_2/HCO_3^- causes pH_i to fall rapidly. Thus, when perfusing single gastric glands as in Figure 3A (22), using the

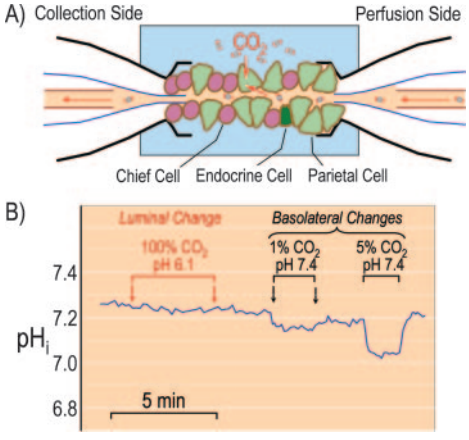

Figure 3. Effect of luminal *versus* basolateral CO_2/HCO_3^- on pH_i in a parietal cell of an isolated, perfused gastric gland. (A) Perfusion of an isolated gastric gland. One pipette was used to bore a hole through the blind end of the gland. (B) Experimental record from a parietal cell. Unless otherwise indicated, the solutions were buffered with HEPES and contained no CO_2 or HCO_3^-. pH_i was measured with the fluorescent dye BCECF and a digital imaging system. Data from reference (24).

technique that was introduced originally by Burg *et al.* (23), we were surprised by the parietal cell data in Figure 3B (and chief cell data; data not shown), which demonstrate that adding CO_2/HCO_3^- to the luminal perfusate causes no detectable pH_i change, even though far lower $[CO_2]$ levels—when presented to the basolateral surface—evoke easily detectable pH_i decreases (24). The perfusate with 100% CO_2 maintained its acidity along the entire length of the lumen, ruling out the possibility that the CO_2 had totally escaped in the first few milliseconds of its journey. Furthermore, luminal CO_2/HCO_3^- failed to alter pH_i over a wide range of $[CO_2]/[HCO_3^-]$ ratios, ruling out the possibility that the separate influxes of CO_2 and HCO_3^- might have precisely compensated for one another and yielded a null pH_i shift. These were the first membranes shown to have negligible gas permeability. We also found that lowering luminal pH to 1 failed to alter pH_i (22).

We similarly observed null pH_i shifts, rather than the expected pH_i increase, when perfusing lumens of gastric gland (24) or colonic crypts (25) with NH_3/NH_4^+. Kikeri *et al.* (26), when perfusing the lumen of a mouse medullary thick ascending limb with NH_3/NH_4^+, previously observed a substantial and paradoxic pH_i decline, which proves that the pH_i effects of the NH_4^+ influx overwhelmed those (if any) of an NH_3 influx. In fact, it would be interesting to see whether the apical membranes of the medullary thick ascending limb, like those of the gastric gland, indeed are impermeable to CO_2 and NH_3.

AQP1: A Bifunctional Water/Gas Channel

In a seminar at the University of Pennsylvania, in which I presented the data in Figure 3B, I suggested that the unknown specialization of gastric-gland apical membranes that allows them to resist luminal pH values below 1 also renders these membranes impermeable to CO_2 and NH_3. Paul De Weer asked me whether I had considered the possibility that the difference between apical and basolateral gastric-gland membranes might be that the basolateral membranes possess "gas channels" that the apical membranes lack. At first blush, I thought that the gas-channel suggestion was outlandish. De Weer soon forgot his comment, but I did not. After returning home, I began to imagine where gas channels might exist, if they existed at all. As luck would have it, Peter Agre, after a seminar at Yale, had generously sent us the cDNA encoding AQP1—discovered in red blood cells (RBC)—so that we might confirm the observation (27) that the water channel AQP1 is not permeable to H^+ (see also reference [28]). The combination of De Weer's comment and Agre's seminar provoked us to think about why RBCs—which transport gas, not water, for a living—should be such a rich reservoir of AQP1. Although there is no doubt that AQP1 is a water channel, might its physiologic role in RBCs be as a gas channel?

To test this hypothesis, Nazih Nakhoul injected cRNA encoding human AQP1 (or water as a control) into *Xenopus* oocytes, which he later injected with CA II protein. The purpose of the CA II was to catalyze the intracellular reaction $CO_2 + H_2O \rightarrow HCO_3^- + H^+$ and thereby keep $[CO_2]$ low near the inner surface of the cell membrane, maximizing the CO_2 influx. Nakhoul found that when he exposed oocytes to CO_2/HCO_3^-, those that expressed AQP1 exhibited a CO_2-induced fall in pH_i that was 40% faster than the control cells (29). This was the first evidence that the presence of a protein could enhance the movement of a dissolved gas across a cell membrane.

Gordon Cooper extended Nakhoul's observations in experiments such as those shown in Figure 4. An important difference in Cooper's experiments is that, rather than inject CA II, he enhanced CO_2 influx by removing the oocyte's vitelline membrane (30). Focusing on the purple record in Figure 4, we see that switching the extracellular solution from one buffered with HEPES to one buffered with 1.5% CO_2/10 mM HCO_3^- caused pH_i to fall slowly, at a rate of -9.6×10^{-4} pH units/s. When Cooper subsequently transferred the oocyte to deionized water, osmosis caused it to lyse in 180 s. This oocyte had a relatively low level of AQP1 expression. The oocyte that is represented by the orange record had a much higher rate of acidification and a more rapid lysis. Finally, the oocyte that is represented by the green record had an even higher acidification rate and an even quicker lysis. These results showed that CO_2 entry paralleled AQP1 expression. Cooper additionally demonstrated that p-chloromercuribenzene sulfonate (pCMBS), an organic mercurial that blocks AQP1's water permeability, also eliminates the statistical difference between AQP1 and control oocytes. Finally, Cooper found that the C189S mutant, which Preston *et al.* (31) showed to be mercury insensitive in terms of water permeability, also is pCMBS insensitive in terms of CO_2 permeability.

Prasad *et al.* (32) confirmed that AQP1 enhances CO_2 permeability, studying purified AQP1 protein that was reconstituted into vesicle that was made from *Escherichia coli* membranes. Yang *et al.* (33) published experiments that seem to disprove the hypothesis that AQP1 acts as a conduit for CO_2. However, as discussed by Cooper *et al.* (34), these experiments were designed in a way that precluded detection of any enhancement of CO_2 permeability by AQP1.

Using a mass-spectroscopy technique to measure the permeability of RBC to $^{12}C^{18}O^{16}O$, Forster *et al.* (35) in 1998 made the

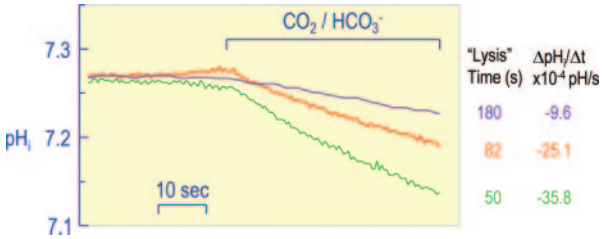

Figure 4. Effect of AQP1 expression on the rate of CO_2-induced acidification in *Xenopus* oocytes. The three records come from experiments on three different *Xenopus* oocytes, with vitelline membranes removed. pH_i was measured with a liquid-membrane pH microelectrode in conjunction with a KCl-filled microelectrode. During the indicated period, the CO_2/HCO_3^--free HEPES solution was replaced with 1.5% CO_2/10 mM HCO_3^- at a fixed pH of 7.50. The lysis time refers to the length of time required for the oocyte to begin to ooze when placed in deionized water. $\Delta pH_i/\Delta t$ is the slope of the CO_2-induced acidification (pH units/s). Data from reference (30).

intriguing observation that 4,4′-diisothiocyanatostilbene-2,2′-disulfonate (DIDS)—which, among other things, blocks the Cl-HCO_3 exchanger AE1—greatly reduces CO_2 permeability. In 2003, Blank and Ehmke (36), using the fluorescent dye BCECF to monitor pH in RBC ghosts, showed that $HgCl_2$ (presumably by blocking AQP1) and DIDS (presumably by blocking AE1) greatly reduced CO_2 permeability. Also in 2003, Uehlein *et al.* (37) demonstrated that a homologue of AQP1 enhances CO_2 permeability in plants, enhancing photosynthesis (the rate-limiting step for which is the availability of CO_2) and the growth of leaves. More recently, Gros *et al.* (38), using the mass-spectroscopy approach with normal and AQP1-null human RBCs, found that AQP1 is responsible for approximately 60% of the cells' CO_2 permeability. An unidentified RBC protein, possibly the Rh complex or AE1, is responsible for an additional approximately 30%. It is interesting that parallel experiments on oocytes showed that DIDS blocks approximately 50% of the CO_2 flux through AQP1.

A final example of a physiologic role for AQP1 as a gas channel is provided by Zhou *et al.* (39), who worked with PT from *wt versus* AQP1-null mice (generously provided by Alan Verkman). Zhou *et al.* found that lack of AQP1 leads to a substantial deficit in HCO_3^- reabsorption, as would be predicted by the model in Figure 1. He also performed another set of experiments that rely on a novel rapid-mixing technique that was developed by Zhao *et al.* (40) for creating out-of-equilibrium (OOE) CO_2/HCO_3^- solutions. We describe this approach in more detail below. When Zhou perfused the PT lumen with a CO_2/HCO_3^--free solution and exposed the basolateral surface to a "pure" HCO_3^- solution (*i.e.*, one with a physiologic [HCO_3^-] and pH but virtually no CO_2), it made no difference whether the PT was from a *wt* or AQP1-null mouse: The backflux of "carbon" was the same. However, when he exposed the basolateral surface to a "pure" CO_2 solution (*i.e.*, one with a physiologic [CO_2] and pH but virtually no HCO_3^-), the backflux, compared with *wt* tubules, was 60% lower in AQP1-null than in wild-type tubules. These data are consistent with the hypothesis that the CO_2 permeability of AQP1 plays a major role in the reabsorption of HCO_3^-.

A lingering issue has been whether it is reasonable to expect a dissolved gas such as CO_2 to pass through AQP1. Recent molecular dynamics simulations by Wang *et al.* (41) suggested that CO_2 could pass (*1*) through each of the four aquapores of an AQP1 tetramer, single file with water and (*2*) through the central pore formed by the four monomers. This central pore seems to be a vacuum through which CO_2 and O_2 can move with great speed.

Apical H^+ Secretion

The NH_4^+ Prepulse

From his original work on the membrane-permeability properties of *Spirogyra* in the late 19th century, Overton understood that NH_3 in a solution that contains NH_4^+ ($NH_3 + H^+ \rightleftarrows NH_4^+$)—as well as various neutral amines ($R\text{-}NH_2 + H^+ \rightleftarrows R\text{-}NH_3^+$) in solutions that contain their charged ammonium ions—crosses cell membranes predominantly in their uncharged form. Working with *Rhododendron* flower petals (the pigment of which shifts from red to blue in response to alkalinity) and starfish eggs that contain neutral red, Jacobs (42) in 1922 recognized that the influx of NH_3—even in acidic solutions of NH_4Cl—causes a rise in pH (Figure 5A). Many decades later, Thomas (17) used a pH-sensitive microelectrode to monitor the rise in pH_i that was caused by exposing a snail neuron to a solution that contained NH_4Cl. The left side of Figure 5B shows an experiment from 1976 in which Boron and De Weer (18) exposed a squid giant axon for a relatively brief period to a solution that contained 10 mM NH_4Cl. Although the NH_3 in the solution was present at very low levels compared with the NH_4^+, the influx of this NH_3 nevertheless led to a consumption of cytoplasmic H^+ and thus an increase in pH_i. Removing the NH_4Cl caused the pH_i changes to reverse. However, pH_i always fell to a value slightly below the initial one.

The explanation for the pH_i undershoot in the first part of the experiment becomes clear with a more protracted exposure to NH_4Cl. The rapid initial NH_3-induced pH_i increase was followed by a much slower but sustained pH_i decrease, which reflects the influx of the weak acid NH_4^+. Subsequently removing the NH_4Cl, after this long exposure, caused pH_i to undershoot the pre-NH_4Cl value by an exaggerated amount. The magnitude of this undershoot reflects the degree of NH_4^+ influx during the previous NH_4Cl exposure. This was the first example of what has come to be known as the "ammonium prepulse" technique for acid loading cells. In fact, the axon will use its pH_i-regulatory machinery to recover from the intracellular acid load in Figure 5B but only in the presence of CO_2/HCO_3^-, as Boron and De Weer (43) subsequently demonstrated. This later work was the first practical use of an NH_4^+ prepulse as a tool to acid load a cell and the first demonstration

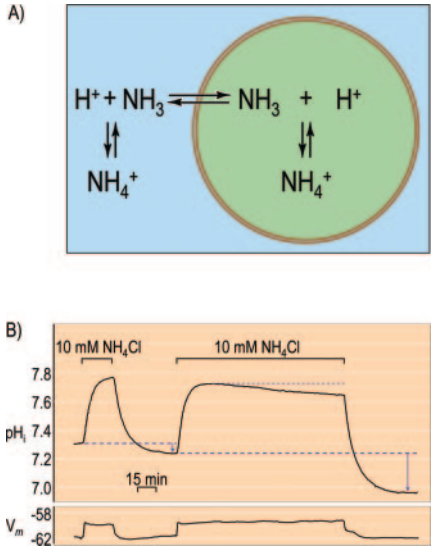

Figure 5. Effect of NH_3/NH_4^+ on pH_i, the NH_4^+ prepulse. (A) Model of NH_3 equilibration across the cell membrane. (B) Experimental record from a squid giant axon. The axon was cannulated at either end, and a glass, pH-sensitive microelectrode was inserted from one end, and a KCl-filled microelectrode was inserted from the other. Data from reference (18).

that cells can use HCO_3^- uptake to neutralize an acid load and thereby regulate pH_i.

Apical Na-H Exchange

One of the first vertebrate cells to be the focus of a study that exploited the NH_4^+ prepulse technique was the PT of the salamander. Figure 6 shows the results of an experiment by Boron and Boulpaep (44), performed on an isolated, perfused tubule, cells of which were impaled with microelectrodes for monitoring pH_i and basolateral membrane potential (basolateral V_m). At first, both the lumen and the "bath" (*i.e.*, the basolateral solution) contained a Na^+-free solution to block Na^+-dependent processes for regulating pH_i. In addition, the bath contained 4-acetamido, 4′-isothiocyanato-2,2′-stilbene disulfonate (SITS; an analog of DIDS) to block the electrogenic Na/HCO_3 co-transporter on the basolateral membrane. Applying NH_4^+ caused a rapid rise in pH_i, followed by a slower fall. Washing away the NH_4^+ caused pH_i to fall substantially and then recover only very slightly. Subsequently returning 100 mM Na^+ to the lumen caused pH_i to return to its initial value. Other experiments showed that this pH_i recovery is inhibited by amiloride, demonstrating that it was an apical Na-H exchanger that was responsible for the pH_i recovery. Murer *et al.* (45), in their studies of brush border membrane vesicles, had been the first to observe Na-H exchange. The groups of Aronson (46) and Saktor (47) also made seminal contributions to our understanding of Na-H exchange by working with brush border membrane vesicles. The experiment shown Figure 6 was the first demonstration of apical Na-H exchange by a living epithelial cell.

Basolateral Na/HCO_3 Co-Transport

Initial Description

In the late 1970s and early 1980s, the mechanism of HCO_3^- exit across the PT basolateral membrane was a subject of considerable interest (reviewed in references [2,3]). One suggestion was that HCO_3^- exited *via* Cl-HCO_3 exchange, although the dominant view seems to have been that HCO_3^- exited *via* a conductive pathway, the simplest explanation for which would be a HCO_3^- channel. While exploring these options in an isolated, perfused salamander PT, Boulpaep and Boron (48) found that lowering basolateral $[HCO_3^-]$ ($[HCO_3^-]_B$) at a fixed $[CO_2]_B$ causes pH_i to fall rapidly—an observation that was consistent with both models. In addition, they found that this maneuver causes basolateral V_m to shift rapidly in the positive direction, consistent with the HCO_3^--conductance model. However, when they removed basolateral Na^+, they made a startling observation (Figure 7): Although pH_i fell as expected (*e.g.*, reversing the basolateral Na-H exchanger would have caused an internal acidification), the basolateral V_m shifted rapidly in the positive direction. Lowering the concentration of an extracellular cation should have caused basolateral V_m to shift in the negative direction. The observation that lowering $[HCO_3^-]_B$ and removing basolateral Na^+ each caused basolateral V_m to shift in the positive direction—together with other data—pointed to a new kind of transporter, an electrogenic Na/HCO_3 co-transporter that moves more negative charge as HCO_3^- (or $CO_3^=$) ions than positive charge as Na^+. Like the previously discovered Cl-HCO_3 exchanger of RBCs and the Na^+-driven Cl-HCO_3 exchanger of invertebrates, the Na/HCO_3 co-transporter is blocked by the disulfonic stilbenes SITS and DIDS. However, in contrast to the other two transporters, the electrogenic Na/HCO_3 co-transporter is independent of Cl^-. Later work by Soleimani and Aronson on basolateral membrane vesicles from rabbit renal cortex pointed to a Na^+:HCO_3^- stoichiometry of 1:3 (49), which ensures that the transporter normally mediates the exit of Na^+ and HCO_3^- across the basolateral membrane—the basolateral step of HCO_3^- reabsorption. Later work by Frömter and his colleagues (50–52) showed that the electrogenic Na/HCO_3 co-transporter is the dominant basolateral pathway for HCO_3^- in the S1 and S2 segments of the PT, where the vast majority of the HCO_3^- reabsorption occurs, but that a basolateral Cl-HCO_3 exchanger also is important in the S3 segment.

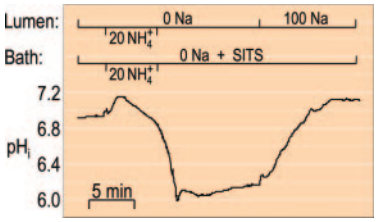

Figure 6. Use of an NH_4^+ prepulse to acid-load an isolated, perfused salamander PT cell. pH_i was measured with a recessed-tip glass pH microelectrode (17), in conjunction with a KCl-filled microelectrode. The tubule was exposed throughout the experiment, at both the luminal and the basolateral sides, to HEPES-buffered solution that lacked CO_2/HCO_3^-. During the indicated time, the tubule was exposed from both the luminal and the basolateral (*i.e.*, "bath") surfaces to a solution in which 20 mM NH_4^+ replaced 20 mM Na^+, an NH_4^+ prepulse designed to acid-load the cell. Extracellular $[Na^+]$ was either 0 or 100 mM, as indicated. V_m, basolateral membrane potential; SITS, 4-acetamido, 4′-isothiocyanato-2,2′-stilbene disulfonate. Data from reference (44).

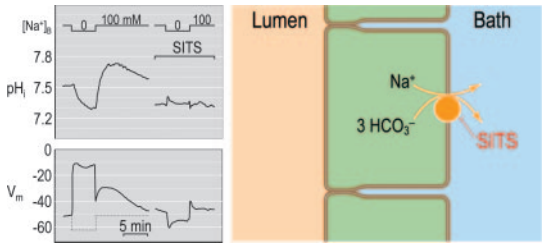

Figure 7. The effect of basolateral Na^+ removal in an isolated, perfused salamander PT, the electrogenic Na/HCO_3 co-transporter. pH_i was measured with a recessed-tip glass pH microelectrode (17), in conjunction with a KCl-filled microelectrode. The tubule was exposed throughout the experiment, at both the luminal and the basolateral sides, to a solution buffered with 1.5% CO_2/10 mM HCO_3^-. During the indicated times, basolateral Na^+ was replaced with an organic cation. Dotted red lines indicate expected V_m response in the absence of an electrogenic Na/HCO_3 co-transporter. Data from reference (48).

Cloning

The absence of a naturally abundant and highly enriched source of the electrogenic Na/HCO_3 co-transporter—unlike the $Cl\text{-}HCO_3$ exchanger AE1, which is highly expressed in RBCs—frustrated early attempts to obtain the cDNA that encodes the electrogenic Na/HCO_3 co-transporter. Michael Romero joined our laboratory in 1992 with the goal of expression-cloning the transporter in *Xenopus* oocytes. Matthias Hediger in the laboratory of Ernest Wright had perfected this approach in cloning the Na/glucose transporter (53–55). Later, as an independent investigator, Hediger had already expression-cloned a wide range of membrane proteins, including a glutamate transporter (56), a subunit of heteromeric amino-acid transporters (57), a urea transporter (58), and an H-driven peptide transporter (59). We were most fortunate that Hediger was interested in collaborating with Romero.

The first step in expression cloning is to inject size-selected mRNA from a tissue source (rabbit kidneys in our case) into *Xenopus* oocytes and then assay for expression of the desired function. Unfortunately, repeated attempts with rabbit mRNA were fruitless. Before giving up, we decided to inject mRNA from salamander kidneys, reasoning that amphibian oocytes might better express an amphibian mRNA. To our delight, this approach was successful. Another key element in this study was our assay. We chose to remove extracellular Na^+ in the presence of CO_2/HCO_3^- and then look for a small, positive shift in V_m that is characteristic of the co-transporter (Figure 7), rather than the usual negative shift. With Hediger, Romero generated a cDNA library from the salamander mRNA and methodically searched through ever-smaller groups of clones to arrive at a single clone that can serve as the template for cRNA that encodes the protein that we named NBC, for Na^+ bicarbonate co-transporter (60).

We anticipated that NBC could be genetically related to any of several known transporters, including the Na/glutamate transporters (subsequently grouped as part of the SLC1 family of solute-linked carriers [61]), the $Cl\text{-}HCO_3$ exchangers AE1 through 3 (now part of the SLC4 family [11]), the Na/monocarboxylate co-transporters (which turned out to be part of the SLC5 family that includes the Na/glucose co-transporters [62]), the Na/bile-salt transporters (SLC10 [63]), the cation-coupled Cl^- co-transporters such as the Na/Cl co-transporter (SLC12 family [64]), the Na/carboxylate co-transporters (SLC13 [65]), and the Na/phosphate co-transporters (SLC17 and SLC34 [66,67]). Upon sequencing the cDNA clone that encodes NBC, we were surprised to learn that the deduced amino-acid sequence of salamander NBC is approximately 30% identical to that for the three anion exchangers AE1 though AE3, which group closely in the dendrogram in Figure 8 (blue region) and also are known as SLC4A1 through SLC4A3. The cloning of the original NBC (also now known as SLC4A4) led to the discovery of several other Na^+-coupled members of the SLC4 family, which group together in the gray region of Figure 8.

Burnham *et al.* (68) subsequently cloned human ortholog of the salamander NBC, and Romero *et al.* (69) obtained the rat clone. It is interesting to note that even the pure rat clone failed to express robustly in *Xenopus* oocytes until subcloned into a

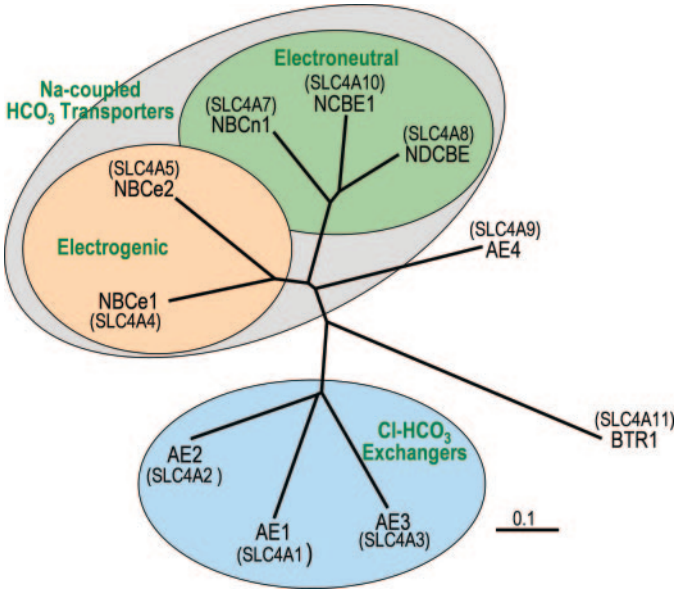

Figure 8. Dendrogram of the SLC4 family of HCO_3^- transporters. All of the transporters are members of the SLC4 family.

Xenopus expression vector that flanks both the 5′ and 3′ ends of the rat NBC with the corresponding untranslated regions of the *Xenopus* β-globin mRNA. This result probably explains why we and others failed in our attempts to expression clone NBCe1 using mammalian mRNA. Bernhard Schmitt raised the first antibodies to the electrogenic NBC, and he and his colleagues demonstrated that the protein is expressed heavily at the basolateral membranes of the S1 and likely the early S2 segments of the renal PT (70).

Other Members of the SLC4 Family

With the discovery of at least one electroneutral NBC—the clone was identified by Pushkin *et al.* (71), and the encoded protein was characterized as an electroneutral NBC by Choi *et al.* (72)—we appended the suffix "e" to designate electrogenic and "n" to designate electroneutral. Moreover, Virkki *et al.* (73) and Sassani *et al.* (74) demonstrated that one of four cDNA clones that previously were isolated by Pushkin *et al.* (75,76) actually encodes a second electrogenic NBC. Thus, the original, renal electrogenic NBC is known as NBCe1-A. A second splice variant of the same gene—identified by Abuladze *et al.* (77) in pancreas and by Choi *et al.* (78) in heart—is known as NBCe1-B. This splice variant seems to be the most widely expressed NBCe1 variant. A brain-specific splice variant that was identified by Bevensee *et al.* (79) is known as NBCe1-C. The second electrogenic NBC gene is NBCe2, and the electroneutral NBC is NBCn1.

In addition to NBCn1, at least two other electroneutral Na^+-coupled HCO_3^- transporters exist. NDCBE, cloned and characterized by Grichtchenko *et al.* (80), is a Na^+-driven $Cl\text{-}HCO_3$ exchanger that is expressed heavily in brain but also in other tissues, including kidney. NCBE, cloned by Wang *et al.* (81), is electroneutral, but whether it transports Cl^- still is controversial. Form follows function among mammalian transporters

Na^+-coupled HCO_3^- transporters, with the electrogenic NBC grouping together in the peach-colored subregion in the dendrogram in Figure 8 and the electroneutral Na^+-coupled HCO_3^- transporters grouping together in the green subregion.

Two members of the SLC4 family have deduced amino acid sequences that lie apart from the rest. AE4 originally was named as a Cl-HCO_3 exchanger (82). However, its function is unsettled, and key areas of its amino acid sequence are more reminiscent of a Na^+-coupled HCO_3^- transporter. BTR1, originally cloned by Parker *et al.* (83), seems to be a Na^+-coupled borate (*i.e.*, boron!) transporter (84), renamed NaBC1. Human mutations in NaBC1 cause a corneal condition that is known as congenital hereditary endothelial dystrophy (85).

Structure

Figure 9 is a model of the topology of NBCe1-A, based on studies of the Cl-HCO_3 exchanger AE1 (86). All members of the family have a large cytoplasmic N terminus (Nt) and a much smaller cytoplasmic C terminus (Ct). The crystal structure of most of the Nt of AE1 has been solved (87) and shows that the Nt is a dimer. We now have crystallized the Nt of NBCe1-A, and a preliminary x-ray diffraction analysis indicates that this Nt, too, is a dimer (88).

Various approaches (*e.g.*, see references [89,90]) generally have yielded similar conclusions about the amino acid residues that contribute to transmembrane segments 1 through 5 (TM1 through TM5). Therefore, investigators feel reasonably confident about these assignments. However, investigators are far less comfortable about the topology of the remainder of the molecule because the data sometimes are conflicting, presumably because the later TMs are more flexible.

One characteristic of the Na^+-coupled HCO_3^- transporters is that they all have a long extracellular loop between TM5 and TM6 (11). Moreover, this loop is the site of consensus glycosylation sites—proved in the case of NBCe1-A (91). Another curiosity is the four heavily conserved cysteine residues in these loops but not those of other SLC4 family members. (It is interesting that AE4 has these for Cys residues.) Work on AE1 shows that lysine residues near the end of TM5 and TM12 can bind covalently the inhibitor DIDS. Preliminary work from our laboratory (92) indicates that these same regions are important for the reversible, noncovalent binding of DIDS.

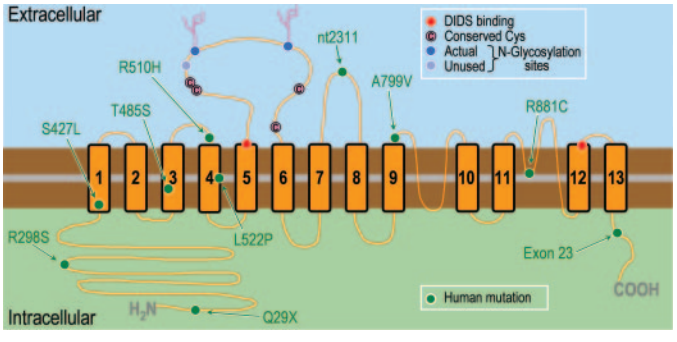

Figure 9. Hypothetical topology of NBCe1-A, based on model of AE1 by Zhu *et al.* (86). The red circles indicate sites of reversible 4,4′-diisothyocyanatostilbene-2,2′-disulfonate (DIDS) binding; the brown circles with "C" indicate Cys residues on the third extracellular loop that are conserved among all Na^+-coupled HCO_3^- transporters; the blue circles indicate actual N-glycosylation sites; the checkered circle indicates an unused consensus glycosylation site; and the green circles indicate the positions of known human mutations.

Naturally Human Mutations of NBCe1 (SLC4A4)

Investigators thus far have identified 10 mutations (94–100) in the human SLC4A4 gene that are associated with a variety of defects that may include severe autosomal recessive, pRTA, ocular abnormalities, growth and mental retardation, and abnormal dentition. The sites of these mutations are indicated by green circles in Figure 9. Three of these are nonsense mutations that lead to premature truncation of the protein, and seven are missense mutations.

Of the three missense mutations, the first is Q29X (95), numbered for the renal splice variant NBCe1-A, which results in a truncation very early in the cytoplasmic Nt. The second is the deletion of nucleotide 2311 (97), which presumably causes a frameshift in codon 721 and, after 27 anomalous amino acids, a premature stop in the extracellular loop between TM7 and TM8. The third missense mutation is a 67-nucleotide deletion at the boundary of exon 23 and the following intron (100); it would lead to a truncated cytoplasmic Ct.

Of the seven missense mutations, R298S in the cytoplasmic Nt, S427L in TM1, and R510H near the extracellular end of TM4 all seem to reduce targeting of the co-transporter to the basolateral membrane in polarized renal epithelial cells in culture (101). All three also exhibit decreased functional expression in *Xenopus* oocytes, although it is not clear to what extent this effect reflects decreased protein delivery to the plasma membrane (94,96,98,101,102).

Work from our laboratory suggests that R881C most likely causes a trafficking defect with normal intrinsic function (103), and A799V seems to cause defects in both trafficking and intrinsic function (104). The most recently discovered NBCe1 mutation is L522P in TM4, which does not traffic to the plasma membrane in oocytes (99).

Basolateral CO_2 and HCO_3^- Sensors

Initial Hints

More than a half century ago, Brazeau and Gilman (105) and Pitts and his colleagues (106) published classical experiments demonstrating that respiratory acidosis elicits a rapid, compen-

satory increase in renal H^+ secretion. However, the problem of determining how the kidney senses acid-base disturbances had been refractory to further dissection, mainly because the equilibrium $CO_2 + H_2O \rightleftarrows HCO_3^- + H^+$ makes it difficult to attribute effects to changes in $[CO_2]$ or to $[HCO_3^-]$ or to $[H^+]$. We became interested in this problem in a very indirect way.

Figure 10 shows the arrangement of an isolated, perfused PT. Figure 11 shows two experiments in which Nakhoul *et al.* (107) used the absorbance spectrum of a fluorescein dye to monitor pH_i in the cells of an isolated, perfused S3 segment of a rabbit PT. In Figure 11A, switching only the luminal buffer from HEPES to CO_2/HCO_3^- caused the expected decrease in pH_i: The influx of CO_2 produced the initial pH_i decline, and the efflux of HCO_3^- across the basolateral membrane sustained the intracellular acidification. In Figure 11B, we see that making the same solution change on the basolateral side has a very different effect. For a few seconds, pH_i declined rapidly, as it did when we added CO_2/HCO_3^- to the lumen. However, within 5 s, pH_i began a rapid increase to a value that is far higher than the initial pH_i. One might argue that the sustained pH_i increase could have been due to HCO_3^- uptake. However, adding basolateral CO_2/HCO_3^- triggers a similar pH_i increase even when CO_2/HCO_3^- is already present in the lumen, and under these conditions, the tubule actively reabsorbs HCO_3^-. That is, the net traffic of HCO_3^- across the basolateral membrane is outward. Therefore, as unlikely as it seems, CO_2 and/or HCO_3^- on the basolateral side of the cell somehow must trigger the secretion of H^+ across the membrane on the apical side.

Further experiments by Chen and Boron (108,109) showed that adding CO_2/HCO_3^- to the bath or to the bath and the lumen markedly stimulated both apical Na-H exchangers and proton pumps. However, adding CO_2/HCO_3^- to the only lumen was without effect. These experiments directly demonstrated that a sensor for CO_2 and/or HCO_3^-—located at or near the basolateral membrane—can stimulate H^+ extrusion at the opposite side of the cell. These experiments provided another surprise: Decreases in pH_i produce only very small increases in the rates of apical Na-H exchange and H^+ pumping in a living PT cell. The real regulation of H^+ transport rates comes not from intracellular protons but from basolateral CO_2 and/or HCO_3^-. But which?

OOE CO_2/HCO_3^- Solutions

In the 1993 paper by Nakhoul *et al.* (107) is an appendix that analyzes the CO_2/HCO_3^--induced alkalinization of Figure 11B in the context of the reactions that are responsible for the interconversion of CO_2 and HCO_3^-. The first of these reactions is very slow, and the second is extremely fast:

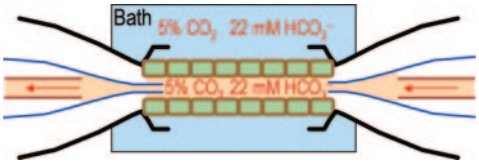

Figure 10. Isolated perfused PT.

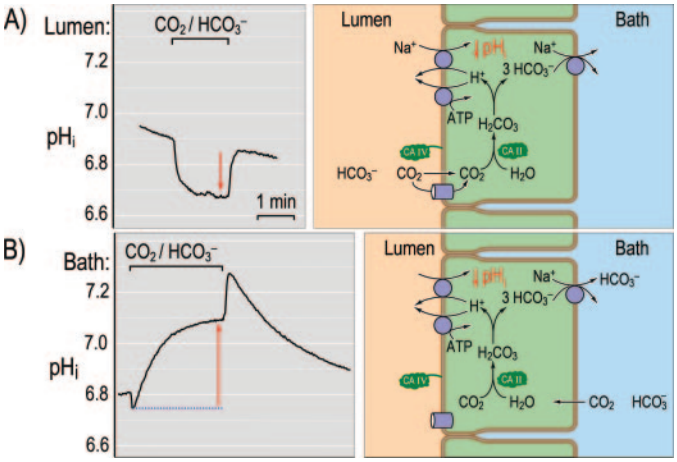

Figure 11. Effect of apical *versus* basolateral CO_2/HCO^-_3 on pH_i in an isolated, perfused rabbit S3 PT. (A) Effect of adding 5% CO_2/25 mM HCO^-_3 to the lumen. (B) Effect of adding 5% CO_2/25 mM HCO^-_3 to the basolateral side (bath). pH_i was computed from the absorbance spectrum of a fluorescein dye. Except as indicated, the luminal and basolateral solutions were buffered with HEPES and contained no CO_2/HCO^-_3. The time bar applies to both panels. Data from reference (107).

$$CO_2 + H_2O \underset{k_{-1}}{\overset{k_1}{\rightleftarrows}} H_2CO_3 \underset{k_{-2}}{\overset{k_2}{\rightleftarrows}} HCO_3^- + H^+$$

Before submitting the paper, I wanted to review my calculations with Robert Berliner, who at the time was Professor Emeritus in our department. After considering the above reaction rates for a couple of hours—and thinking about Figure 11B—Bob wistfully looked up at the ceiling and said that it was too bad that we had to add CO_2 and HCO_3^- together, rather than one at a time. In an instant—primed by our discussion of the slow reaction governed by k_1 and k_{-1}—the thought came to me, "Of course we can!" All we need to do is to take advantage of that slow reaction . . . and thus were born out-of-equilibrium (OOE) solutions.

Figure 12A shows the approach for generating a solution with physiologic levels of HCO_3^- and pH but virtually no CO_2 ("pure" HCO_3^-), and Figure 12B shows the comparable approach for generating a solution with physiologic levels of CO_2 and pH but virtually no HCO_3^- ("pure" CO_2). However, implementing OOE solutions proved to be more challenging than conceiving of them. Shortly after my conversation with Bob, Jinhua Zhao arrived as a new postdoctoral fellow. For 2 yr, she: (*1*) labored with ever more powerful syringe pumps to deliver evenly two streams of liquid, (*2*) employed various tricks for adequately mixing these two streams, (*3*) dealt with issues of temperature regulation, and (*4*) accomodated the chemistry of CO_2 and HCO_3^-. We tested the system on squid giant axons (40), in which we were able to create "pure" CO_2 solutions that could acidify the cell and increase intracellular buffering power as predicted as well as "pure" HCO_3^- solutions that could supply the substrate for a HCO_3^- transporter but not increase intracellular buffering power.

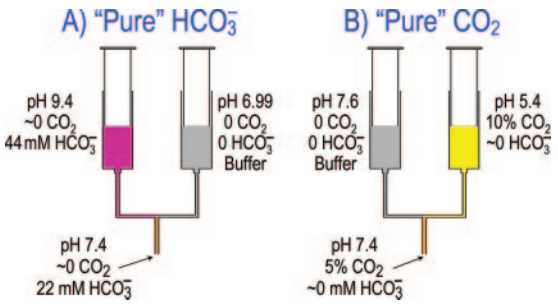

Figure 12. Generating out-of-equilibrium (OOE) CO_2/HCO_3^- solutions. (A) "Pure" HCO_3^-. (B) "Pure" CO_2. In each case, a single syringe pump is used to deliver solutions evenly from two syringes. The two solutions meet at a "T" that is filled with a nylon mesh that promotes mixing. The total flow typically is 7 ml/min. The time from mixing to delivery of the OOE solution to the tubule to the removal of the solution is approximately 200 ms. Thus, the tubule is exposed continuously to a newly generated solution.

Zhao also applied her new technology to the isolated perfused rabbit PT (110) and then introduced Yuehan Zhou to the project. He monitored $JHCO_3$ as well as the rate of volume absorption (J_V) as he systematically used OOE solutions to vary basolateral composition one parameter at a time (Figure 13A). The results show that raising $[HCO_3^-]_B$ (at a fixed $[CO_2]_B$ of 5% and a fixed pH_B of 7.40) causes $JHCO_3$ to fall (Figure 13B, left)—an appropriate response for the "metabolic" part of metabolic acid-base disturbances. That is, the greater the plasma $[HCO_3^-]$, the less HCO_3^- the kidney ought to reabsorb. Moreover, raising $[CO_2]_B$ (at a fixed $[HCO_3^-]_B$ of 22 mM and a fixed pH_B of 7.40) causes $JHCO_3$ to rise (Figure 13B, middle)—an appropriate compensation for the "respiratory" part of respiratory acid-base disturbances. That is, the greater the plasma $[CO_2]$, the more HCO_3^- the kidney ought to reabsorb. However, we were surprised to find that raising pH_B (at a fixed $[HCO_3^-]_B$ of 22 mM and a fixed $[CO_2]_B$ of 5%) elicits no change in $JHCO_3$ (Figure 13B, right).

In parallel experiments, we measured pH_i under the conditions of Figure 13B and found that, indeed, pH_i changes substantially as one increases pH_B from 6.8 to 8.0. However, these changes in pH_B and pH_i do not evoke changes in $JHCO_3$. Instead, at least in terms of its acute response to acid-base disturbances, the PT regulates plasma pH not by monitoring pH but by monitoring two surrogates: the main buffer components of the body, HCO_3^- and CO_2 (Figure 14). This tactic of regulating a parameter that the body does not measure directly is not unique to acid-base parameters and the PT. For example, the body uses stretch receptors in vessels to gauge the adequacy of the effective circulating blood volume.

An extremely interesting observation in the above study is that the changes in $JHCO_3$ occurred without the expected parallel changes in J_V. Because the fluid that the PT reabsorbs is approximately isosmotic, an increase in $JHCO_3$, for example, should have been accompanied by a sizable increase in J_V. It seems that the PT cell compensates for changes in $NaHCO_3$ reabsorption by making reciprocal changes in the reabsorption of other solutes, thereby keeping J_V relatively constant (Figure 14). This response would help to maintain a stable BP as the tubule responds to acid-base disturbances.

It is worth noting that in the above experiments, we applied the challenges only to the basolateral surface of the tubule. Therefore, it is possible that PT have a pH sensor at the apical

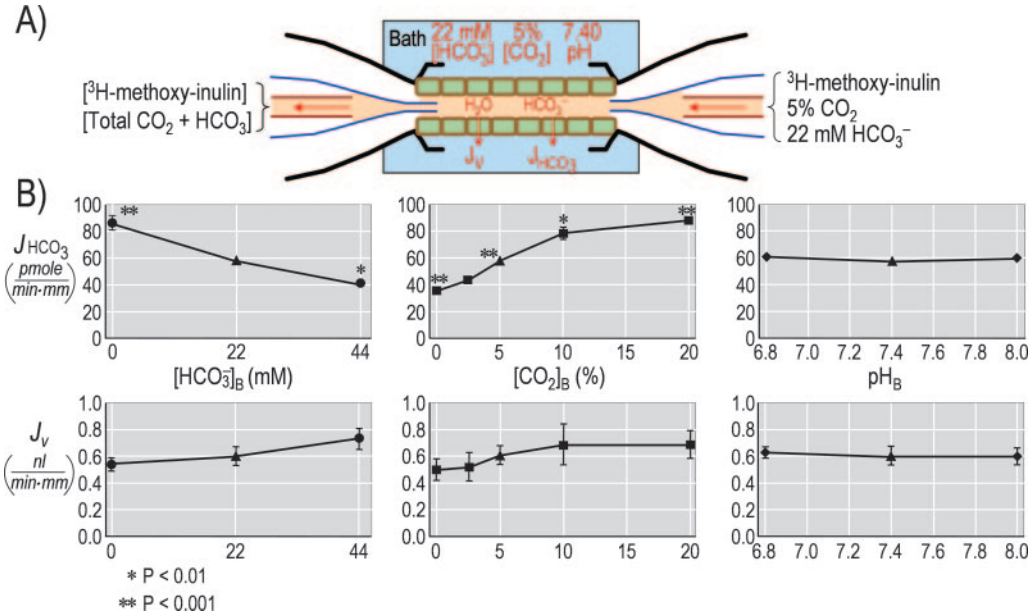

Figure 13. Effect on HCO_3^- reabsorption of varying—one at a time—basolateral $[HCO_3^-]$, $[CO_2]$, and pH. (A) Model. (B) Experimental data obtained on isolated perfused rabbit S2 PT. The triangles indicate standard equilibrated conditions (5% CO_2, 22 mM HCO_3^-, pH 7.40). All other symbols represent OOE solutions. $JHCO_3$, rate of HCO_3^- reabsorption; J_V, rate of volume reabsorption; $_B$, basolateral. Data from reference (142).

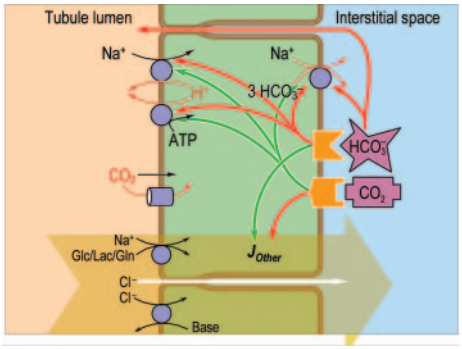

Figure 14. Model of the regulation of $JHCO_3$ and J_V by basolateral CO_2 and HCO_3^- in a renal PT. The green arrows represent stimulation, and the red arrows represent inhibition. We propose that basolateral CO_2 stimulates the acid-base transporters but reciprocally inhibits the transporters that are responsible for the reabsorption of other solutes. HCO_3^- would have the opposite effect. Glc, glucose; Lac, lactate; Gln, glutamine; J_{Other}, rate of reabsorption of solutes other than $NaHCO_3$.

membrane. Also, the above experiments were acute: The tubule acclimated for approximately 5 min in the test solution, and the entire period of data collection lasted approximately 30 min. Alpern and colleagues showed that cultured PT cells that were subjected for 2 d to either metabolic or respiratory acidosis responded by increasing their activity of Na-H exchange, a process that requires new protein synthesis (111). Moreover, this effect, as well as increased expression of NHE3 mRNA, is blocked by overexpressing Csk (112), a natural inhibitor of src kinases.

Role of Tyrosine Kinases

A critical question is how the tubule is able to sense changes in $[CO_2]_B$ and transduce them into altered cell function. The bacterium *Rhizobium meliloti* senses O_2 (113) and the plant *Arabidopsis thaliana* senses ethylene (114–119) using membrane proteins that signal through a histidine kinase. Because animal cells lack histidine kinases, we hypothesized that PT cells might use a tyrosine kinase to signal an increase in CO_2. Indeed, as shown in Figure 15, 35 nM PD168393, which alkylates a Cys residue in the ATP binding pocket of tyrosine kinases in the erbB family (120), eliminates the ability of the PT to respond to

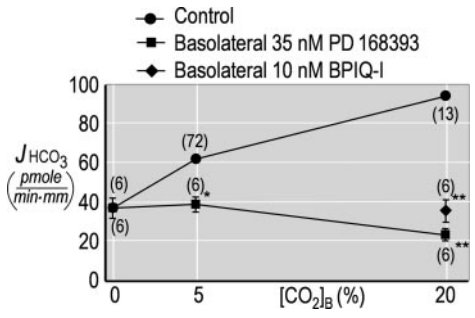

Figure 15. Effect of tyrosine-kinase inhibitors on the CO_2-induced increase in $JHCO_3$. Data from reference (121).

changes in $[CO_2]_B$ (121). Similarly, 10 nM BPIQ-I, which also targets members of the erbB family (122), blocks the ability of the tubule to respond to increased $[CO_2]_B$. Indeed, preliminary work suggests that exposing tubule suspensions to CO_2/HCO_3^- leads to the phosphorylation of erbB1 (*i.e.*, EGF receptor) at Tyr residues (123). Although we do not yet know the molecule that senses CO_2, it seems that this dissolved gas signals through a receptor tyrosine kinase, perhaps in part through erbB1.

Role of Angiotensin II

The hormone that has the greatest stimulatory effect on $JHCO_3$ is angiotensin II (AngII), applied at a "low" dosage to either the luminal or basolateral surface (124–127). When applied at a "high" dosage to either surface, however, AngII actually reduces $JHCO_3$ (126,128).

We examined the effect low-dosage (10^{-11} M) and of high-dosage (10^{-9} M) AngII on the response of $JHCO_3$ to alterations in $[CO_2]_B$ (129). We found that low-dosage AngII, added to either the lumen or the bath, tends to shift the $JHCO_3$-*versus*-$[CO_2]_B$ relationship to the left, so that lower levels of $[CO_2]_B$ tend to stimulate HCO_3^- reabsorption. Conversely, high-dosage AngII, added to either the lumen or the bath, tends to blunt the $JHCO_3$-*versus*-$[CO_2]_B$ relationship.

The PT has all of the molecular machinery to generate its own AngII (130–136), which actually appears in the tubule lumen. It is not yet established whether the tubule secretes angiotensinogen, AngI, or AngII. However, preliminary data from our group on Prinivil, an inhibitor of the angiotensin-converting enzyme, suggest that the tubule actually secretes preformed AngII (137). We decided to examine the effect of AngII receptor blockers on the $JHCO_3$-*versus*-$[CO_2]_B$ relationship. We were surprised to find that in the absence of added AngII, 10^{-8} saralasin, a peptide that blocks both AT_1 and AT_2 receptors, reduces $JHCO_3$ to levels that normally are observed at 0% CO_2 (see Figure 13B) and renders the tubule insensitive to changes in $[CO_2]_B$ between 0 and 20%. The AT_1-specific blocker candesartan has a similar effect. Finally, in tubules from AT_{1A}-null mice, we find a moderate depression of $JHCO_3$ at 5% CO_2 and a total insensitivity to changes in $[CO_2]_B$.

Endogenous luminal AngII plays at least a critical permissive role in the tubule's response to alterations in $[CO_2]_B$. It would be interesting to know whether basolateral CO_2 somehow accentuates the endogenous AngII system, perhaps by increasing the secretion of AngII, increasing the density or the sensitivity of apical AT_1 receptors, or enhancing downstream signaling from the AT_1 receptor to the acid-base transporters.

Conclusions and Outlook

Looking back over the past 60 yr of progress in understanding acid secretion by the PT, it is sobering to realize that the pioneers in the field, working with technologies that are far more primitive than those that are at our disposal today, were able to assemble a good picture of the fundamental processes (138–141): The tubule exchanges luminal Na^+ for cytosolic H^+, carbonic anhydrase catalyzes the secreted H^+ to titrate filtered HCO_3^- to CO_2 and H_2O, and these substances enter the cell

and regenerate HCO_3^- that then moves into the blood. Today, we understand many more of the details, including the dynamics of electrical and chemical gradients and the molecular identities of the transporters. We know their amino acid sequences, and we even know many examples in which specific mutations of these proteins lead to human disease.

These advances notwithstanding, much remains to be learned. We still do not understand how the transporters function at an atomic level or the mechanisms of disease-causing mutations. Such understanding will come eventually through advances in structural biology. However, reading between the lines of this review, one can sense that many mysteries remain even at the cellular and molecular levels. Just how do CO_2 and other gases move through aquaporins and other gas channels? Which molecules does the PT cell use to sniff basolateral CO_2 and HCO_3^-? How does the cell transduce these signals to the acid-base transporters? How does the cell reciprocally regulate the reabsorption of $NaHCO_3$ and of other solutes so as to stabilize J_V? What role does locally generated AngII play in these processes? How does the PT cell integrate information from CO_2 levels, locally *versus* systemically generated AngII, and other hormones such as parathyroid hormone and endothelin? With continued support from the National Institutes of Health and other agencies and the enthusiasm of bright young scientists, the renal community can look forward to the day when other winners of the Homer W. Smith Award will answer these questions.

Acknowledgments

The preparation of this review was supported by National Institutes of Health grants DK30344 and DK17433.

I thank the National Institutes of Health for 25 yr of support. I also thank agencies such as the American Heart Association and the National Kidney Foundation for supporting my research and the careers of fellows in my laboratory. I thank Duncan Wong for computer support and Charleen Bertolini for administrative support.

References

1. Alpern RJ: Cell mechanisms of proximal tubule acidification. *Physiol Rev* 70: 79–114, 1990
2. Warnock DG, Rector FC Jr: Proton secretion by the kidney. *Annu Rev Physiol* 41: 197–210, 1979
3. Rector FC: Sodium, bicarbonate, and chloride absorption by the proximal tubule. *Am J Physiol* 244: F461–F471, 1983
4. Sly WS, Hu PY: Human carbonic anhydrases and carbonic anhydrase deficiencies. *Annu Rev Biochem* 64: 375–401, 1995
5. Wakabayashi S, Shigekawa M, Pouyssegur J: Molecular physiology of vertebrate Na+/H+ exchangers. *Physiol Rev* 77: 51–74, 1997
6. Counillon L, Pouyssegur J: The expanding family of eucaryotic Na(+)/H(+) exchangers. *J Biol Chem* 275: 1–4, 2000
7. Donowitz M, Cha BY, Zachos NC, Brett CL, Sharma A, Tse CM, Li XH: NHERF family and NHE3 regulation. *J Physiol (Lond)* 567: 3–11, 2005
8. Weinman EJ, Cunningham R, Shenolikar S: NHERF and regulation of the renal sodium-hydrogen exchanger NHE3. *Pflugers Arch* 450: 137–144, 2005
9. Gluck SL, Lee BS, Wang SP, Underhill D, Nemoto J, Holliday LS: Plasma membrane V-ATPases in proton-transporting cells of the mammalian kidney and osteoclast. *Acta Physiol Scand Suppl* 643: 203–212, 1998
10. Paroutis P, Touret N, Grinstein S: The pH of the secretory pathway: Measurement, determinants, and regulation. *Physiology (Bethesda)* 19: 207–215, 2004
11. Romero MF, Fulton CM, Boron WF: The SLC4 family of HCO3− transporters. *Pflugers Arch* 447: 495–509, 2004
12. Seki G, Coppola S, Yoshitomi K, Christina Burckhardt BC, Samarzija I, Muller-Berger S, Fromter E: On the mechanism of bicarbonate exit from renal proximal tubular cells. *Kidney Int* 49: 1671–1677, 1996
13. Agre P: Nobel lecture. Aquaporin water channels. *Biosci Rep* 24: 127–163, 2004
14. Giebisch G, Windhager EE: Transport of acids and bases. In *Medical Physiology. A Cellular and Molecular Approach*, edited by Boron WF, Boulpaep EL, Philadelphia, Elsevier Saunders, 2005, pp 845–860
15. Jacobs MH: To what extent are the physiological effects of carbon dioxide due to hydrogen ions? *Am J Physiol* 51: 321–331, 1920
16. Roos A, Boron WF: Intracellular pH. *Physiol Rev* 61: 296–434, 1981
17. Thomas RC: Intracellular pH of snail neurones measured with a new pH-sensitive glass micro-electrode. *J Physiol (Lond)* 238: 159–180, 1974
18. Boron WF, De Weer P: Intracellular pH transients in squid giant axons caused by CO2, NH3 and metabolic inhibitors. *J Gen Physiol* 67: 91–112, 1976
19. Thomas RC: The effect of carbon dioxide on the intracellular pH and buffering power of snail neurones. *J Physiol (Lond)* 255: 715–735, 1976
20. Boron WF: Intracellular pH transients in giant barnacle muscle fibers. *Am J Physiol* 233: C61–C73, 1977
21. Bevensee MO, Alper SL, Aronson PS, Boron WF: Control of intracellular pH. In: *The Kidney, Physiology and Pathophysiology*, edited by Seldin DW, Giebisch G, New York, Raven, 2000, pp 391–442
22. Waisbren SJ, Geibel JP, Boron WF, Modlin IM: Luminal perfusion of isolated gastric glands. *Am J Physiol* 266: C1013–C1027, 1994
23. Burg M, Grantham J, Abramow M, Orloff J: Preparation and study of fragments of single rabbit nephrons. *Am J Physiol* 210: 1293–1298, 1966
24. Waisbren SJ, Geibel JP, Modlin IM, Boron WF: Unusual permeability properties of gastric gland cells. *Nature* 368: 332–335, 1994
25. Singh SK, Binder HJ, Geibel JP, Boron WF: An apical permeability barrier to NH3/NH4+ in isolated, perfused colonic crypts. *Proc Natl Acad Sci U S A* 92: 11573–11577, 1995
26. Kikeri D, Sun A, Zeidel ML, Hebert SC: Cell membranes impermeable to NH3. *Nature* 339: 478–480, 1989
27. Zeidel ML, Nielsen S, Smith BL, Ambudkar SV, Maunsbach AB, Agre P: Ultrastructure, pharmacologic inhibition, and transport selectivity of aquaporin channel-forming integral protein in proteoliposomes. *Biochemistry* 33: 1606–1615, 1994
28. Murata K, Mitsuoka K, Hirai T, Walz T, Agre P, Heymann

JB, Engel A, Fujiyoshi Y: Structural determinants of water permeation through aquaporin-1. *Nature* 407: 599–605, 2000
29. Nakhoul NL, Davis BA, Romero MF, Boron WF: Effect of expressing the water channel aquaporin-1 on the CO2 permeability of *Xenopus* oocytes. *Am J Physiol* 274: C543–C548, 1998
30. Cooper GJ, Boron WF: Effect of pCMBS on CO2 permeability of *Xenopus* oocytes expressing aquaporin 1 or its C189S mutant. *Am J Physiol* 275: C1481–C1486, 1998
31. Preston GM, Jung JS, Guggino WB, Agre P: The mercury-sensitive residue at cysteine 189 in the CHIP28 water channel. *J Biol Chem* 268: 17–20, 1993
32. Prasad GV, Coury LA, Fin F, Zeidel ML: Reconstituted aquaporin 1 water channels transport CO2 across membranes. *J Biol Chem* 273: 33123–33126, 1998
33. Yang B, Fukuda N, Van Hoek A, Matthay MA, Ma T, Verkman AS: Carbon dioxide permeability of aquaporin-1 measured in erythrocytes and lung of aquaporin-1 null mice and in reconstituted liposomes. *J Biol Chem* 275: 2686–2692, 2000
34. Cooper GJ, Zhou Y, Bouyer P, Grichtchenko II, Boron WF: Transport of volatile solutes through AQP1. *J Physiol* 542: 17–29, 2002
35. Forster RE, Gros G, Lin L, Ono Y, Wunder M: The effect of 4,4′-diisothiocyanato-stilbene-2,2′-disulfonate on CO2 permeability of the red blood cell membrane. *Proc Natl Acad Sci U S A* 95: 15815–15820, 1998
36. Blank ME, Ehmke H: Aquaporin-1 and HCO_3−-Cl− transporter-mediated transport of CO2 across the human erythrocyte membrane. *J Physiol (Lond)* 550: 419–429, 2003
37. Uehlein N, Lovisolo C, Siefritz F, Kaldenhoff R: The tobacco aquaporin NtAQP1 is a membrane CO2 pore with physiological functions. *Nature* 425: 734–737, 2003
38. Endeward V, Musa-Aziz R, Cooper GJ, Chen L, Pelletier MF, Virkki LV, Supuran CT, King LS, Boron WF, Gros G: Evidence that aquaporin 1 is a major pathway for CO2 transport across the human erythrocyte membrane. *FASEB J* 2006, in press
39. Zhou Y, Bouyer P, Boron WF: Evidence that AQP1 is a functional CO2 channel in proximal tubules [Abstract]. *FASEB J* 20: A1225, 2006
40. Zhao J, Hogan EM, Bevensee MO, Boron WF: Out-of-equilibrium CO2/HCO3− solutions and their use in characterizing a new K/HCO3 cotransporter. *Nature* 374: 636–639, 1995
41. Wang Y, Schulten K, Tajkhorshid E: Channel mediated gas transport across lipid membranes [Abstract]. *Biophys J* 20: 1375, 2006
42. Jacobs MH: The influence of ammonium salts on cell reaction. *J Gen Physiol* 5: 181–188, 1922
43. Boron WF, De Weer P: Active proton transport stimulated by CO2/HCO3− blocked by cyanide. *Nature* 259: 240–241, 1976
44. Boron WF, Boulpaep EL: Intracellular pH regulation in the renal proximal tubule of the salamander. Na-H exchange. *J Gen Physiol* 81: 29–52, 1983
45. Murer H, Hopfer U, Kinne R: Sodium/proton antiport in brush-border-membrane vesicles isolated from rat small intestine and kidney. *Biochem J* 154: 597–604, 1976
46. Kinsella JL, Aronson PS: Properties of the Na+-H+ exchanger in renal microvillus membrane vesicles. *Am J Physiol* 238: F461–F469, 1980
47. Freiberg JM, Kinsella J, Sacktor B: Glucocorticoids increase the Na+-H+ exchange and decrease the Na+ gradient-dependent phosphate-uptake systems in renal brush border membrane vesicles. *Proc Natl Acad Sci U S A* 79: 4932–4936, 1982
48. Boron WF, Boulpaep EL: Intracellular pH regulation in the renal proximal tubule of the salamander: Basolateral HCO3− transport. *J Gen Physiol* 81: 53–94, 1983
49. Soleimani M, Grassl SM, Aronson PS: Stoichiometry of Na+-HCO3− cotransport in basolateral membrane vesicles isolated from rabbit renal cortex. *J Clin Invest* 79: 1276–1280, 1987
50. Kondo Y, Fromter E: Axial heterogeneity of sodium-bicarbonate cotransport in proximal straight tubule of rabbit kidney. *Pflugers Arch* 410: 481–486, 1987
51. Kondo Y, Fromter E: Evidence of chloride bicarbonate exchange mediating bicarbonate efflux from S3 segments of rabbit renal proximal tubule. *Pflugers Arch* 415: 726–733, 1990
52. Seki G, Fromter E: The chloride base exchanger in the basolateral cell-membrane of rabbit renal proximal tubule S3 segment requires bicarbonate to operate. *Pflugers Arch* 417: 37–41, 1990
53. Hediger MA: High resolution preparative gel electrophoresis of DNA fragments and plasmid DNA using a continuous elution apparatus. *Anal Biochem* 159: 280–286, 1986
54. Hediger MA, Coady MJ, Ikeda TS, Wright EM: Expression cloning and cDNA sequencing of the Na+/glucose cotransporter. *Nature* 330: 379–381, 1987
55. Hediger MA, Ikeda T, Coady M, Gundersen CB, Wright EM: Expression of size-selected mRNA encoding the intestinal Na/glucose cotransporter in *Xenopus laevis* oocytes. *Proc Natl Acad Sci U S A* 84: 2634–2637, 1987
56. Kanai Y, Hediger MA: Primary structure and functional characterization of a high-affinity glutamate transporter. *Nature* 360: 467–471, 1992
57. Wells RG, Hediger MA: Cloning of a rat kidney cDNA that stimulates dibasic and neutral amino acid transport and has sequence similarity to glucosidases. *Proc Natl Acad Sci U S A* 89: 5596–5600, 1992
58. You G, Smith CP, Kanai Y, Lee WS, Stelzner M, Hediger MA: Cloning and characterization of the vasopressin-regulated urea transporter. *Nature* 365: 844–847, 1993
59. Fei YJ, Kanai Y, Nussberger S, Ganapathy V, Leibach FH, Romero MF, Singh SK, Boron WF, Hediger MA: Expression cloning of a mammalian proton-coupled oligopeptide transporter. *Nature* 368: 563–566, 1994
60. Romero MF, Hediger MA, Boulpaep EL, Boron WF: Expression cloning and characterization of a renal electrogenic Na+/HCO3− cotransporter. *Nature* 387: 409–413, 1997
61. Kanai Y, Hediger MA: The glutamate/neutral amino acid transporter family SLC1: Molecular, physiological and pharmacological aspects. *Pflugers Arch* 447: 469–479, 2004
62. Wright EM, Turk E: The sodium/glucose cotransport family SLC5. *Pflugers Arch* 447: 510–518, 2004
63. Hagenbuch B, Dawson P: The sodium bile salt cotransport family SLC10. *Pflugers Arch* 447: 566–570, 2004
64. Hebert SC, Mount DB, Gamba G: Molecular physiology of

cation-coupled Cl- cotransport: The SLC12 family. *Pflugers Arch* 447: 580–593, 2004
65. Markovich D, Murer H: The SLC13 gene family of sodium sulphate/carboxylate cotransporters. *Pflugers Arch* 447: 594–602, 2004
66. Reimer RJ, Edwards RH: Organic anion transport is the primary function of the SLC17/type I phosphate transporter family. *Pflugers Arch* 447: 629–635, 2004
67. Murer H, Forster I, Biber J: The sodium phosphate cotransporter family SLC34. *Pflugers Arch* 447: 763–767, 2004
68. Burnham CE, Amlal H, Wang Z, Shull GE, Soleimani M: Cloning and functional expression of a human kidney Na+:HCO3− cotransporter. *J Biol Chem* 272: 19111–19114, 1997
69. Romero MF, Fong P, Berger UV, Hediger MA, Boron WF: Cloning and functional expression of rNBC, an electrogenic Na+-HCO3− cotransporter from rat kidney. *Am J Physiol* 274: F425–F432, 1998
70. Schmitt BM, Biemesderfer D, Romero MF, Boulpaep EL, Boron WF: Immunolocalization of the electrogenic Na+/HCO3− cotransporter in mammalian and amphibian kidney. *Am J Physiol* 276: F27–F36, 1999
71. Pushkin A, Abuladze N, Lee I, Newman D, Hwang J, Kurtz I: Cloning, tissue distribution, genomic organization, and functional characterization of NBC3, a new member of the sodium bicarbonate cotransporter family. *J Biol Chem* 274: 16569–16575, 1999
72. Choi I, Aalkjaer C, Boulpaep EL, Boron WF: An electroneutral sodium/bicarbonate cotransporter NBCn1 and associated sodium channel. *Nature* 405: 571–575, 2000
73. Virkki LV, Wilson DA, Vaughan-Jones RD, Boron WF: Functional characterization of human NBC4 as an electrogenic Na+-HCO3− cotransporter (NBCe2). *Am J Physiol Cell Physiol* 282: C1278–C1289, 2002
74. Sassani P, Pushkin A, Gross E, Gomer A, Abuladze N, Dukkipati R, Carpenito G, Kurtz I: Functional characterization of NBC4: A new electrogenic sodium- bicarbonate cotransporter. *Am J Physiol Cell Physiol* 282: C408–C416, 2002
75. Pushkin A, Abuladze N, Newman D, Lee I, Xu G, Kurtz I: Cloning, characterization and chromosomal assignment of NBC4, a new member of the sodium bicarbonate cotransporter family. *Biochim Biophys Acta* 1493: 215–218, 2000
76. Pushkin A, Abuladze N, Newman D, Lee I, Xu G, Kurtz I: Two C-terminal variants of NBC4, a new member of the sodium bicarbonate cotransporter family: Cloning, characterization, and localization. *IUBMB Life* 50: 13–19, 2000
77. Abuladze N, Lee I, Newman D, Hwang J, Boorer K, Pushkin A, Kurtz I: Molecular cloning, chromosomal localization, tissue distribution, and functional expression of the human pancreatic sodium bicarbonate cotransporter. *J Biol Chem* 273: 17689–17695, 1998
78. Choi I, Romero MF, Khandoudi N, Bril A, Boron WF: Cloning and characterization of a human electrogenic Na+-HCO3− cotransporter isoform (hhNBC). *Am J Physiol* 276: C576–C584, 1999
79. Bevensee MO, Schmitt BM, Choi I, Romero MF, Boron WF: An electrogenic Na/HCO3 cotransporter (NBC) with a novel C terminus, cloned from rat brain. *Am J Physiol Cell Physiol* 278: C1200–C1211, 2000
80. Grichtchenko II, Choi I, Zhong X, Bray-Ward P, Russell JM, Boron WF: Cloning, characterization, and chromosomal mapping of a human electroneutral Na+-driven Cl-HCO3 exchanger. *J Biol Chem* 276: 8358–8363, 2001
81. Wang CZ, Yano H, Nagashima K, Seino S: The Na+-driven Cl−/HCO3− exchanger: Cloning, tissue distribution, and functional characterization. *J Biol Chem* 275: 35486–35490, 2000
82. Tsuganezawa H, Kobayashi K, Iyori M, Araki T, Koizumi A, Watanabe SI, Kaneko A, Fukao T, Monkawa T, Yoshida T, Kim DK, Kanai Y, Endou H, Hayashi M, Saruta T: A new member of the HCO3− transporter superfamily is an apical anion exchanger of beta-intercalated cells in the kidney. *J Biol Chem* 276: 8180–8189, 2000
83. Parker MD, Ourmozdi EP, Tanner MJ: Human BTR1, a new bicarbonate transporter superfamily member and human AE4 from kidney. *Biochem Biophys Res Commun* 282: 1103–1109, 2001
84. Park M, Li Q, Shcheynikov N, Zeng WZ, Muallem S: NaBC1 is a ubiquitous electrogenic Na+-coupled borate transporter essential for cellular boron homeostasis and cell growth and proliferation. *Mol Cell* 16: 331–341, 2004
85. Vithana EN, Morgan P, Sundaresan P, Ebenezer ND, Tan DTH, Mohamed MD, Anand S, Khine KO, Venkataraman D, Yong VHK, Salto-Tellez M, Venkatraman A, Guo K, Hemadevi B, Srinivasan M, Prajna V, Khine M, Casey JR, Inglehearn CF, Aung T: Mutations in sodium-borate cotransporter SLC4A11 cause recessive congenital hereditary endothelial dystrophy (CHED2). *Nat Genet* 38: 755–757, 2006
86. Zhu Q, Lee DW, Casey JR: Novel topology in C-terminal region of the human plasma membrane anion exchanger, AE1. *J Biol Chem* 278: 3112–3120, 2003
87. Zhang D, Kiyatkin A, Bolin JT, Low PS: Crystallographic structure and functional interpretation of the cytoplasmic domain of erythrocyte membrane band 3. *Blood* 96: 2925–2933, 2000
88. Gill HS, Boron WF: Preliminary X-ray diffraction analysis of the cytoplasmic N-terminal domain of the Na/HCO3 cotransporter NBCe1-A. *Acta Crystallograph Sect F Struct Biol Cryst Commun* 62: 534–537, 2006
89. Kuma H, Shinde AA, Howren TR, Jennings ML: Topology of the anion exchange protein AE1: The controversial sidedness of lysine 743. *Biochemistry* 41: 3380–3388, 2002
90. Cheung JC, Cordat E, Reithmeier RA: Trafficking defects of the Southeast Asian ovalocytosis deletion mutant of anion exchanger 1 membrane proteins. *Biochem J* 392: 425–434, 2005
91. Choi I, Hu L, Rojas JD, Schmitt BM, Boron WF: Role of glycosylation in the renal electrogenic Na+-HCO3− cotransporter (NBCe1). *Am J Physiol Renal Physiol* 284: F1199–F1206, 2003
92. Lu J, Virkki LV, Choi I, Boulpaep EL, Boron WF: The effect of mutations of K559 and K562, within the KMIK motif of TM5, on the DIDS sensitivity of the electrogenic Na/HCO3 cotransporter from human kidney (hNBCe1-A) [Abstract]. *FASEB J* 17: A1221, 2003
93. Abuladze N, Azimov R, Newman D, Liu W, Tatishchev S, Pushkin A, Kurtz I: Critical amino acid residues involved in the electrogenic sodium bicarbonate cotransporter kNBC1-mediated transport. *J Physiol* 565: 717–730, 2005
94. Igarashi T, Inatomi J, Sekine T, Cha SH, Kanai Y, Kunimi M, Tsukamoto K, Satoh H, Shimadzu M, Tozawa F, Mori T, Shiobara M, Seki G, Endou H: Mutations in SLC4A4 cause

permanent isolated proximal renal tubular acidosis with ocular abnormalities. *Nat Genet* 23: 264–266, 1999
95. Igarashi T, Inatomi J, Sekine T, Seki G, Shimadzu M, Tozawa F, Takeshima Y, Takumi T, Takahashi T, Yoshikawa N, Nakamura H, Endou H: Novel nonsense mutation in the Na+/HCO3− cotransporter gene (SLC4A4) in a patient with permanent isolated proximal renal tubular acidosis and bilateral glaucoma. *J Am Soc Nephrol* 12: 713–718, 2001
96. Dinour D, Chang MH, Satoh J, Smith BL, Angle N, Knecht A, Serban I, Holtzman EJ, Romero MF: A novel missense mutation in the sodium bicarbonate cotransporter (NBCe1/SLC4A4) causes proximal tubular acidosis and glaucoma through ion transport defects. *J Biol Chem* 279: 52238–52246, 2004
97. Inatomi J, Horita S, Braverman N, Sekine T, Yamada H, Suzuki Y, Kawahara K, Moriyama N, Kudo A, Kawakami H, Shimadzu M, Endou H, Fujita T, Seki G, Igarashi T: Mutational and functional analysis of SLC4A4 in a patient with proximal renal tubular acidosis. *Pflugers Arch* 448: 438–444, 2004
98. Horita S, Yamada H, Inatomi J, Moriyama N, Sekine T, Igarashi T, Endo Y, Dasouki M, Ekim M, Al Gazali L, Shimadzu M, Seki G, Fujita T: Functional analysis of NBC1 mutants associated with proximal renal tubular acidosis and ocular abnormalities. *J Am Soc Nephrol* 16: 2270–2278, 2005
99. Demirci FY, Chang MH, Mah TS, Romero MF, Gorin MB: Proximal renal tubular acidosis and ocular pathology: A novel missense mutation in the gene (SLC4A4) for sodium bicarbonate cotransporter protein (NBCe1). *Mol Vis* 12: 324–330, 2006
100. Igarashi T, Inatomi J, Sekine T, Seki G, Yamada H, Horita S, Fujita T: Mutational and functional analysis of the Na+/HCO3-cotransporter gene (SLC4AC) in patients with permanent isolated proximal renal tubular acidosis and ocular abnormalities [Abstract]. *J Am Soc Nephrol* 14: 302A, 2003
101. Li HC, Szigligeti P, Worrell RT, Matthews JB, Conforti L, Soleimani M: Missense mutations in Na+:HCO3− cotransporter NBC1 show abnormal trafficking in polarized kidney cells: A basis of proximal renal tubular acidosis. *Am J Physiol Renal Physiol* 289: F61–F71, 2005
102. Davis BA, Rojas JD, Virkki LV, Hogan EM, Boron WF: Functional analysis of point mutations in human electrogenic Na/HCO3 cotransporters NBCe1-A and -B [Abstract]. *FASEB J* 16: A796, 2002
103. Toye AM, Parker MD, Daly CM, Lu J, Virkki LV, Pelletier MF, Boron WF: The human NBCe1-A mutant R881C, associated with proximal renal tubular acidosis, retains function but is mistargeted in polarized renal epithelia. *Am J Physiol Cell Physiol* 2006, in press
104. Parker MD, Toye AM, Boron WF: The human NBCe1-A mutant A799V, associated with proximal renal tubular acidosis, exhibits both mistargeting in polarized renal epithelia and reduced intrinsic function [Abstract]. *J Am Soc Nephrol* 2006, in press
105. Brazeau P, Gilman A: Effect of plasma CO2 tension on renal tubular reabsorption of bicarbonate. *Am J Physiol* 175: 33–38, 1953
106. Dorman PJ, Sullivan WJ, Pitts RF: The renal response to acute respiratory acidosis. *J Clin Invest* 33: 82–90, 1954
107. Nakhoul NL, Chen LK, Boron WF: Effect of basolateral CO2/HCO3− on intracellular pH regulation in the rabbit S3 proximal tubule. *J Gen Physiol* 102: 1171–1205, 1993
108. Chen LK, Boron WF: Acid extrusion in S3 segment of rabbit proximal tubule: I. Effect of bilateral CO2/HCO3−. *Am J Physiol* 268: F179–F192, 1995
109. Chen LK, Boron WF: Acid extrusion in S3 segment of rabbit proximal tubule: II. Effect of basolateral CO2/HCO3−. *Am J Physiol* 268: F193–F203, 1995
110. Zhao J, Zhou Y, Boron WF: Effect of isolated removal of either basolateral HCO3− or basolateral CO2 on HCO3− reabsorption by rabbit S2 proximal tubule. *Am J Physiol Renal Physiol* 285: F359–F369, 2003
111. Horie S, Moe O, Tejedor A, Alpern RJ: Preincubation in acid medium increases Na/H antiporter activity in cultured renal proximal tubule cells. *Proc Natl Acad Sci U S A* 87: 4742–4745, 1990
112. Yamaji Y, Amemiya M, Cano A, Preisig PA, Miller RT, Moe OW, Alpern RJ: Overexpression of csk inhibits acid-induced activation of NHE-3. *Proc Natl Acad Sci U S A* 92: 6274–6278, 1995
113. Gilles-Gonzalez MA, Ditta GS, Helinski DR: A haemoprotein with kinase activity encoded by the oxygen sensor of *Rhizobium meliloti*. *Nature* 350: 170–172, 1991
114. Chang C, Kwok SF, Bleecker AB, Meyerowitz EM: *Arabidopsis* ethylene-response gene ETR1: Similarity of product to two-component regulators. *Science* 262: 539–544, 1993
115. Schaller GE, Bleecker AB: Ethylene-binding sites generated in yeast expressing the Arabidopsis ETR1 gene. *Science* 270: 1809–1811, 1995
116. Rodriguez FI, Esch JJ, Hall AE, Binder BM, Schaller GE, Bleecker AB: A copper cofactor for the ethylene receptor ETR1 from Arabidopsis. *Science* 283: 996–998, 1999
117. Clark KL, Larsen PB, Wang X, Chang C: Association of the *Arabidopsis* CTR1 Raf-like kinase with the ETR1 and ERS ethylene receptors. *Proc Natl Acad Sci U S A* 95: 5401–5406, 1998
118. Kieber JJ, Rothenberg M, Roman G, Feldmann KA, Ecker JR: CTR1, a negative regulator of the ethylene response pathway in *Arabidopsis*, encodes a member of the raf family of protein kinases. *Cell* 72: 427–441, 1993
119. Ouaked F, Rozhon W, Lecourieux D, Hirt H: A MAPK pathway mediates ethylene signaling in plants. *EMBO J* 22: 1282–1288, 2003
120. Fry DW, Bridges AJ, Denny WA, Doherty A, Greis KD, Hicks JL, Hook KE, Keller PR, Leopold WR, Loo JA, McNamara DJ, Nelson JM, Sherwood V, Smaill JB, Trumpp-Kallmeyer S, Dobrusin EM: Specific, irreversible inactivation of the epidermal growth factor receptor and erbB2, by a new class of tyrosine kinase inhibitor. *Proc Natl Acad Sci U S A* 95: 12022–12027, 1998
121. Zhou Y, Bouyer P, Boron WF: Role of a tyrosine kinase in the CO2-induced stimulation of HCO3− reabsorption by rabbit S2 proximal tubules. *Am J Physiol Renal Physiol* 291: F358–F367, 2006
122. Rewcastle GW, Palmer BD, Thompson AM, Bridges AJ, Cody DR, Zhou H, Fry DW, McMichael A, Denny WA: Tyrosine kinase inhibitors. 9. Synthesis and evaluation of fuse tricyclic quinazoline analogues as ATP site inhibitors of the tyrosine kinase activity of the epidermal growth factor receptor. *J Med Chem* 39: 918–928, 1996
123. Skelton LA, Bouyer P, Boron WF: CO2/HCO3 induces

EGFR phosphorylation in the proximal tubule [Abstract]. *J Am Soc Nephrol* 2006, in press
124. Garvin JL: Angiotensin stimulates bicarbonate transport and Na+/K+ ATPase in rat proximal straight tubules. *J Am Soc Nephrol* 1: 1146–1152, 1991
125. Liu FY, Cogan MG: Angiotensin II stimulation of hydrogen ion secretion in the rat early proximal tubule. *J Clin Invest* 82: 601–607, 1988
126. Wang T, Chan YL: Mechanism of angiotensin II action on proximal tubular transport. *J Pharmacol Exp Ther* 252: 689–695, 1990
127. Baum M, Quigley R, Quan A: Effect of luminal angiotensin II on rabbit proximal convoluted tubule bicarbonate absorption. *Am J Physiol* 273: F595–F600, 1997
128. Chatsudthipong V, Chan YL: Inhibitory effect of angiotensin II on renal tubular transport. *Am J Physiol Renal Physiol* 260: F340–F346, 1991
129. Zhou Y, Bouyer P, Boron WF: Effects of angiotensin II on the CO2 dependence of HCO3− reabsorption by the rabbit S2 renal proximal tubule. *Am J Physiol Renal Physiol* 290: F666–F673, 2006
130. Ingelfinger JR, Zuo WM, Fon EA, Ellison KE, Dzau VJ: In situ hybridization evidence for angiotensinogen messenger RNA in the rat proximal tubule. An hypothesis for the intrarenal renin angiotensin system. *J Clin Invest* 85: 417–423, 1990
131. Yanagawa N, Capparelli AW, Jo OD, Friedal A, Barrett JD, Eggena P: Production of angiotensinogen and renin-like activity by rabbit proximal tubular cells in culture. *Kidney Int* 39: 938–941, 1991
132. Wang L, Lei C, Zhang SL, Roberts KD, Tang SS, Ingelfinger JR, Chan JS: Synergistic effect of dexamethasone and isoproterenol on the expression of angiotensinogen in immortalized rat proximal tubular cells. *Kidney Int* 53: 287–295, 1998
133. Moe OW, Ujiie K, Star RA, Miller RT, Widell J, Alpern RJ, Henrich WL: Renin expression in renal proximal tubule. *J Clin Invest* 91: 774–779, 1993
134. Marchetti J, Roseau S, Alhenc-Gelas F: Angiotensin I converting enzyme and kinin-hydrolyzing enzymes along the rabbit nephron. *Kidney Int* 31: 744–751, 1987
135. Casarini DE, Boim MA, Stella RC, Schor N: Endopeptidases (kininases) are able to hydrolyze kinins in tubular fluid along the rat nephron. *Am J Physiol Renal Physiol* 277: F66–F74, 1999
136. Navar LG, Harrison-Bernard LM, Wang CT, Cervenka L, Mitchell KD: Concentrations and actions of intraluminal angiotensin II. *J Am Soc Nephrol* 10[Suppl 11]: S189–S195, 1999
137. Zhou Y, Bouyer P, Boron WF: Role of endogenously secreted angiotensin II in the CO2-induced stimulation of HCO3 reabsorption by rabbit S2 proximal tubules [Abstract]. *FASEB J* 18: A1016, 2004
138. Pitts R, Alexander RS: The nature of the renal tubular mechanism for acidifying the urine. *Am J Physiol* 144: 239–254, 1945
139. Pitts RF: Renal excretion of acid. *Fed Proc* 7: 418–426, 1948
140. Berliner RW: Renal secretion of potassium and hydrogen ions. *Fed Proc* 11: 695–700, 1952
141. Berliner RW, Kennedy TJ Jr, Orloff J: Relationship between acidification of the urine and potassium metabolism; effect of carbonic anhydrase inhibition on potassium excretion. *Am J Med* 11: 274–282, 1951
142. Zhou Y, Zhao J, Bouyer P, Boron WF: Evidence from renal proximal tubules that HCO3− and solute reabsorption are acutely regulated not by pH but by basolateral HCO3− and CO2. *Proc Natl Acad Sci U S A* 102: 3875–3880, 2005